minerals

MDPI

Review

C–O Stable Isotope Geochemistry of Carbonate Minerals in the Nonsulfide Zinc Deposits of the Middle East: A Review

Nicola Mondillo [1,*], Maria Boni [1], Michael Joachimski [2] and Licia Santoro [3]

1 Dipartimento di Scienze della Terra, dell'Ambiente e delle Risorse, Università degli Studi di Napoli Federico II, Complesso Universitario di Monte S. Angelo, Via Cintia 21, 80126 Napoli, Italy; boni@unina.it
2 GeoZentrum Nordbayern, University of Erlangen-Nuremberg, Schlossgarten 5, 91054 Erlangen, Germany; michael.joachimski@fau.de
3 Department of Earth Sciences, Natural History Museum, Cromwell Road, London SW7 5BD, UK; licia.santoro85@gmail.com
* Correspondence: nicola.mondillo@unina.it; Tel.: +39-081-2535-067

Received: 3 October 2017; Accepted: 6 November 2017; Published: 10 November 2017

Abstract: Zinc nonsulfides are well represented in the Middle East, with occurrences in Turkey, Iran, and Yemen. Their genesis can be constrained by using carbon and oxygen isotope systematics applied to carbonate minerals. The $\delta^{13}C$ ratios of smithsonite and hydrozincite in Iran and Turkey are comprised in the typical interval of supergene Zn carbonates (−0.4 and −7.1‰ V-PDB). The oxygen isotope geochemistry is more complex. Oxygen isotope compositions of smithsonite of the Hakkari deposit (Turkey) ($\delta^{18}O$ from 24.2 to 25.6‰ V-SMOW) point to precipitation temperatures between ~4 and ~18 °C, corresponding to a normal weathering environment at these latitudes, whereas $\delta^{18}O$ of smithsonite from other Middle East deposits (Angouran in Iran, Jabali in Yemen) point to the precipitation from low- to medium-temperature hydrothermal fluids. The C–O isotopic compositions of hydrozincite from the Mehdi Abad, Irankuh, and Chah-Talkh deposits can be only partially compared with those of smithsonite, because the oxygen isotopes fractionation equation for hydrozincite-water is not known. A comparison between the geochemical characteristics of all Zn-nonsulfide ores in the Middle East indicates that, even though several mineral deposits are derived from supergene weathering processes, other ones have been deposited from fluids associated with magmatic activity (Angouran, Iran) or with hydrothermal systems (Jabali, Yemen). This suggests that it is not possible to apply a common interpretative model to the genesis of all nonsulfide deposits in the Middle East.

Keywords: Zn-nonsulfide deposits; C–O stable isotopes; weathering; Middle East

1. Introduction

Various types of mineral deposits occur in the Middle East, all genetically related to the development of the "Tethyan Metallogenic Belt" and scattered from eastern Turkey to southeastern Iran, as well as in the Arabian Peninsula [1]. The most important mineralization types in this belt are porphyry-Cu and epithermal-Au deposits, skarn, volcanic-hosted massive sulfides, sediment-hosted massive sulfides, and Mississippi Valley-type deposits. Podiform chromite ores, Ni-Co laterites, and bauxites have been also locally identified [1,2]. Along with the above-mentioned ores, the "Zn-nonsulfides" mineralization type is well represented in the entire area, with major occurrences in Iran, Turkey, and Yemen [3–12].

Zinc nonsulfide deposits contain Zn-oxidized minerals, mainly represented by smithsonite, hydrozincite, hemimorphite, sauconite, and willemite [13,14]. These deposits are genetically

distinguished between supergene and hypogene. Supergene nonsulfide mineralizations form through the oxidation of sulfide-bearing ores, under the influence of meteoric waters in a weathering regime [11,14]. The hypogene deposits are instead derived from hydrothermal and/or metamorphic fluids [14]. When mineralogical and petrographic studies alone are not sufficient to reveal their supergene or hypogene origin, stable isotope data of carbonate minerals contained within nonsulfide deposits yield valuable information on the mineralization temperatures, on the origin and evolution of ore-forming fluids, on the mechanisms of ore deposition, and on wall-rock alteration patterns [15]. Oxygen and carbon isotope data of carbonate minerals have already been published for several nonsulfide deposits in the Middle East, as Hakkari in Turkey [8,11], Angouran [4,6], Mehdi Abad [5], Irankuh [5], and Chah-Talkh [16] in Iran, as well as Jabali in Yemen [10] (Figure 1). In this short note, we compare the carbon and oxygen isotope compositions of several nonsulfide Zn deposits and prospects throughout the Middle East. The data are discussed within the metallogenic context of each deposit, and the stable isotope signatures are interpreted as in other Zn(Pb) nonsulfide concentrations known from literature. In this review we will also mention, a few other nonsulfide ores, like several important deposits in Turkey and Iran, where stable isotope measurements are not yet published or not available [17–21].

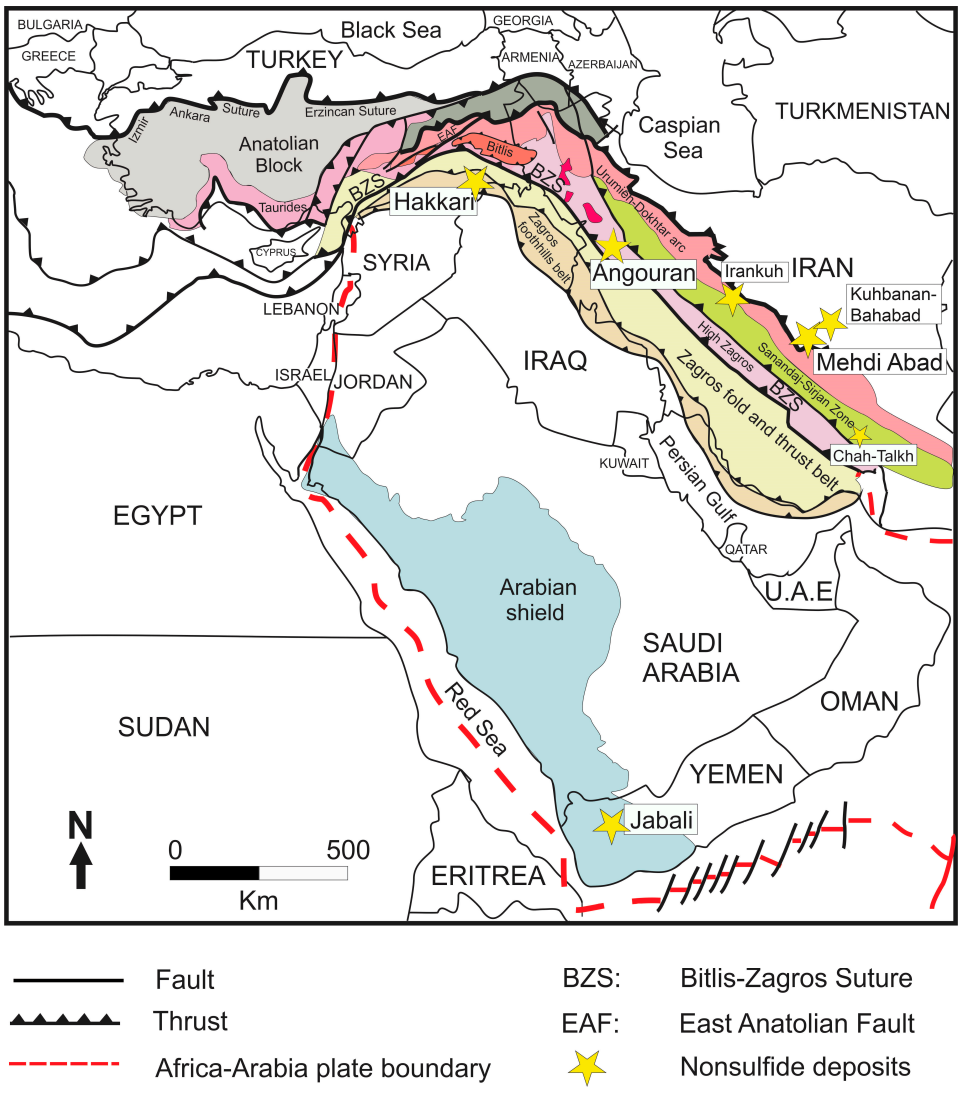

Figure 1. Map of the Middle East region, with major structural units and location of the nonsulfide Zn deposits where C–O stable isotope data have been published.

2. Zinc Nonsulfide Deposits in the Middle East

2.1. Turkey

Nonsulfide Zn(Pb) deposits are known in the Tauride block (southern or central Turkey) and in the Arabian Platform in southeastern Turkey. In the Zamanti district the primary sulfide mineralization, hosted by Devonian-Early Cretaceous carbonates has been almost entirely replaced by a supergene mineral association, mainly consisting of smithsonite, hemimorphite, hydrozincite, Zn-Al-silicates and high amounts of Fe-(hydr)oxides [11,17]. Also the Keban Zn-Pb primary deposit, hosted in Paleozoic marbles, has been oxidized by meteoric waters, resulting in thick horizons of supergene nonsulfide ores, which contain smithsonite, cerussite, and Fe-(hydr)oxides [11,18]. In the Kayseri/Aladağ region, the Horzum Mine near Adana (in Devonian carbonates) was one of the larger operations in the region [2]. In the Tufanbeyli district there are several high-grade smithsonite-rich deposits [2]. Zinc mineralization is hosted here within Middle-to-Upper Devonian limestone and dolomite, with thin sandstone interlayers. Although broadly stratiform, the Tufanbeyli oxidized zinc mineralization is highly irregular on a local scale, both in terms of geometry and grade (Zn ranges between 0.79% and 31.87%) [11].

The Hakkari prospect [7,8,11] is located in southeastern Turkey (Figure 1), a few kilometers south of the Bitlis-Zagros suture [2]. The main project area is positioned within a broad 20 km wide and 100 km long east-west trending belt, extending from 60 km east of Hakkari and Şirnak Provincial boundary. The Hakkari orebodies occur in Middle Triassic to Early Cretaceous sedimentary rocks [19], and the zinc mineralization is hosted in a porous and/or brecciated, karstified limestone, flanked by cherty dolomite. The primary sulfide mineralization has been considered to belong to the Mississippi Valley-type [17], to be a SEDEX- or Irish-type deposit [1], and a distal CRD mineralization (upper Tertiary in age) [7]. The Hakkari nonsulfide Zn(Pb) mineralization formed through oxidation of the primary sulfide deposit. Ore minerals mainly consist of smithsonite and hemimorphite, commonly associated with Fe-Mn-(hydr)oxides. Two smithsonite generations have been identified: the first generation has a massive texture, and replaces primary sphalerite, as well as the carbonate host rock; the second one occurs as globular, perfectly-zoned concretions in druses and cavities. Minor amounts of hemimorphite also occur, and some Zn, associated with As, Sb, and Tl is hosted in the Fe-Mn-(hydr)oxides. Cerussite is the main Pb mineral. Calcite occurs at least in three generations: a first generation, barren of metallic elements representing the host rock; and a second, Pb-bearing one, occurring in veins and as cement of hydrothermal breccias. The third calcite generation (strongly enriched in Cd, Pb, and locally in Zn) has been commonly detected together with smithsonite and hemimorphite [7,8].

2.2. Iran

About 600 Zn(Pb) deposits are presently known in Iran. The most important metallogenetic provinces for nonsulfide Zn mineralization are located in the central part of the country, in the Sanandaj–Sirjan zone, and in the Alborz region. The age of the host rocks ranges from Proterozoic to Tertiary and part of the orebodies are also exploited for sulfides. Only a small amount of nonsulfide zinc deposits is currently in an active mining process, such as Angouran, Iran-Kuh, and Kuh-e-Surmeh. The giant Mehdi Abad deposit is a special case, where both economic sulfide and nonsulfide ores occur [5,11,20,21].

The Mehdi Abad Zn-Pb-(Ag) deposit (Figure 1) is situated in the Yazd Province, approximately 550 km southeast of Tehran. Exploration during the last two decades revealed huge economic reserves (nonsulfides only amounting to 45.2 Mt at 7.15% Zn and 2.47% Pb) [5,20]. Several occurrences have been explored at Mehdi Abad and one of them, called the Calamine mine, has been exploited in historical times [20,21]. In the deposit area, a thick Early Cretaceous sedimentary sequence is exposed, lying unconformably on top of the Jurassic Shir-Kuh granite that initially formed a major palaeo-relief. The Zn-Pb-Ba mineralization of the Mehdi Abad deposit occurs within the

Taft Formation [21], which is part of a large-scale carbonate platform system that characterized the Yazd Block during the Early Cretaceous. The mineralization of Mehdi Abad occurs along two horizons that extend over a length of >4 km. The sulfide and nonsulfide ores of the first ore horizon are hosted by organic matter-rich shale, limestone and dolomite of the Taft Formation, whereas nonsulfide ores (Calamine mine) of the second horizon are enclosed in the overlying Abkuh Formation [5,20]. The Zn(Pb) mineralization consists of smithsonite, hemimorphite, and hydrozincite. Cerussite and anglesite are commonly associated with lenses of residual or supergene galena. The nonsulfide concentrations in the Mehdi Abad deposit can be subdivided into a "red zinc ore" and a "white zinc ore". The red ore is rich in Zn (up to 30%), Fe (17%) and other metals such as Pb and As [5]. In contrast, the white ore shows higher Zn grades (up to 40%) and low concentrations of Fe (<7%), minor Pb and As [5].

The Irankuh district (Figure 1) comprises several Zn(Pb) deposits, located in the Irankuh Mountain Range in west central Iran [5]. The regional stratigraphic sequence in the area starts with Early Jurassic shale, followed by Barremian-Aptian sandstone and limestone, Upper Aptian shale, and on the top of the sequence, Tertiary sediments. Sulfide and nonsulfide mines and prospects occur in this district within the Cretaceous dolomite and limestone: among them the Kolahdarvazeh open pit produces mainly nonsulfide zinc ores [5]. The oxidized part of the Zn, Fe, and Pb ore zones exploited at Kolahdarvazeh occurs not only on the top of the primary ore, but it also represents the infilling within deep karstic cavities in the Cretaceous carbonates [5]. A distinct oscillatory zoning (zinc-enriched and zinc-poor bands) in the Kolahdarvazeh deposit is considered to have been caused by variations of the water table, cyclically altering the regular deepening grade of the oxidation profiles [5].

The Chah-Talkh deposit (Figure 1) is located in the southern Sanandaj–Sirjan Zone of the Zagros orogenic belt, close to the Urumieh–Dokhtar volcanic arc [16]. Nonsulfide zinc minerals are dominated by smithsonite, hemimorphite, and hydrozincite.

Over 40 nonsulfide dominated Zn(Pb) deposits are located in the Kuhbanan–Bahabad area, Central Iran [22]. The host rocks of these deposits are Upper Permian (-Lower Triassic) carbonate rocks. Sphalerite, galena, and pyrite are the main sulfide minerals in the primary assemblage, and the mineralization was considered comparable with known MVT deposits. Smithsonite, hydrozincite, and hemimorphite were deposited in connection with an oxidation stage, together with minor cerussite, anglesite, and wulfenite [22].

The Angouran Zn(Pb-Ag) deposit (Figure 1) is situated in the western Zanjan Province, NW Iran, about 450 km northwest of Tehran, within the northwestern part of the Sanandaj-Sirjan Zone [4,23]. The deposit is hosted by a metamorphic core complex, which consists of amphibolites, serpentinites, gneisses, micaschists, and calcitic and dolomitic marbles. The complex has been rapidly exhumed during an extensional phase in the Lower Miocene [23]. The primary ore deposit formed at a lithological boundary, which comprises a thrust contact between footwall schists and hanging wall marbles. The host marbles have been thrust onto a thick pile of Miocene ignimbrites cut by 10 Ma basaltic dykes. A 10 km long carbonate travertine tongue overlies the Cenozoic volcanic rocks and contains dispersed metal anomalies including Zn and As. The orebody exhibits a vertical zonation with a supergene overprinting, with (i) an underlying Zn-rich hypogene sulfide and mixed sulfide-carbonate ore; and (ii) a carbonate ore towards the top. The field relationship and geology of the area suggest that the primary mineralization is younger than 10 Ma, and also point to a genetic link between the formation of the Zn carbonate ores, travertine deposition, and the geothermal activity. The latter was active at the time of secondary mineralization, and continues to the present in the whole district [4]. Nonsulfide mineralization occurred at Angouran during two successive stages, characterized by a first stage of Zn carbonates (stage I carbonate ore), associated with both preexisting and subordinate newly formed sulfides, and a second stage of supergene carbonates (Zn and minor Pb) coexisting with Fe-hydroxides (stage II carbonate ore) [4].

2.3. Yemen

The Jabali deposit (Figure 1) is located in Yemen, along the western border of the Marib-Al-Jawf/Sab'atayn basin [10,24]. The rock hosting both sulfide and nonsulfide ores is the dolomitized limestone of the Jurassic Shuqra Formation (Amran Group). Smithsonite is the most abundant economic mineral in the nonsulfide part of the deposit, and is associated with minor hydrozincite, hemimorphite, acanthite, and greenockite. The Zn-carbonate occurs in two main generations: smithsonite 1, which replaces both host dolomite and sphalerite, and smithsonite 2, occurring as concretions and vein fillings in the host rock [10]. The nonsulfide mineralization evolved through different stages: (1) alteration of original sulfides; (2) alteration of host rock and formation of Zn-bearing dolomite [25]; (3) partial dissolution and replacement of dolomite and Zn-bearing dolomite by smithsonite 1; (4) precipitation of smithsonite 2 in veins and cavities, together with Ag- and Cd-sulfides.

The most favorable setting for the formation of the Jabali nonsulfides could be placed in early Miocene (~17 Ma), when weathering was favored by major uplift, in association with the main phase of Red Sea extension. Low-temperature hydrothermal fluids may have also circulated at the same time, through a magmatically-induced geothermal activity along the borders of the Marib-Al-Jawf/Sab'atayn basin [10].

3. Materials and Methods

Most information quoted in this study was derived from published data of the numerous papers cited in the references. We tried to avoid unreliable citations and removed from the reference list the occurrences where no stable isotope (C–O) measurements were carried out or the data are unavailable. Stable isotope analyses of the Hakkari carbonates, whose preliminary data have been published in [8], were carried out at the University of Erlangen-Nuremberg (Germany). The analyses have been performed on concretionary smithsonite and sparry calcites genetically associated with smithsonite concretions. Carbonate powders and hand-picked minerals were made to react with phosphoric acid at 70 °C using a Gasbench II connected to a Thermo Finnigan Five Plus mass spectrometer. Carbon and oxygen isotope values are reported in per mil relative to V-PDB and V-SMOW, respectively, by assigning $\delta^{13}C$ and $\delta^{18}O$ values of +1.95 and −2.20‰ V-PDB to NBS19 and −46.6 and −26.7‰ V-PDB to LSVEC, respectively. Reproducibility was checked by replicate analysis of laboratory standards, and was ±0.07‰ (1σ) for both carbon and oxygen isotope analyses. Oxygen isotope values of smithsonite and calcite were corrected using the phosphoric acid fractionation factors given by [15,26,27].

4. Stable Isotopes (C–O) in Nonsulfide Deposits in the Middle East

The carbon and oxygen isotope compositions for zinc carbonates and calcite from Zn nonsulfide deposits in the Middle East are reported in Table 1, and depicted in the diagram of Figure 2, together with the field of Gilg et al. [15], which includes the C–O stable isotopes ratios measured on smithsonite from several supergene nonsulfide Zn deposits in the world (Italy, Poland, Belgium, Portugal, Namibia, New Zealand, Australia). Isotopic values of host rocks carbonates are also reported.

Table 1. Carbon and oxygen isotopes of carbonates in Zn nonsulfide deposits of Middle East.

Locality	Sample n.	Sample Description	$\delta^{13}C$ (‰ VPDB)	$\delta^{18}O$ (‰ VSMOW)
Hakkari, Turkey	H 2061	smithsonite 1	−5.09	24.61
	H 2063	smithsonite 1	−5.06	24.23
	H 2066	smithsonite 1	−3.36	24.51
	H 2066	smithsonite 2	−6.03	25.35
	H 2070	smithsonite 1	−5.80	24.28
	H 2076	calcite (host rock)	−0.66	24.92
	H 2077	calcite (host rock)	−2.54	24.88
	H 2076	calcite (sparry crystals from a vein cutting the host rock)	−1.83	21.63
	H 2077	calcite (sparry crystals from a vein cutting the host rock)	−2.04	21.36
	H 2063	calcite (sparry crystals associated with smithsonite)	−7.35	22.57
	H 2062	calcite (sparry crystals associated with smithsonite)	−5.87	21.48
Mehdi Abad, Iran [5]	M02127	hydrozincite	−1.8	20.4
	M02129	hydrozincite	−0.4	21.9
	M02134	hydrozincite	−3.8	21.5
	M02109	calcite	2.0	16.5
	M02113b	calcite	1.1	15.1
	M02117	calcite	−0.4	21.4
	M02120	calcite	0.7	16.8
	M02109	dolomite	2.9	23.0
	M02129	dolomite	2.6	25.0
	M02113b	limestone	2.8	24.8
	M02120	limestone	2.2	22.4
Kolahdarvazeh, Irankuh, Iran [5]	IK02136	hydrozincite	−3.8	22.4
	IK02129	hydrozincite	−4.3	22.3
	IK02145	hydrozincite	−4.2	21.6
	IK02115	hydrozincite	−4.7	22.9
	IK02134	hydrozincite	−5.7	22.6
	IK02123	hydrozincite	−7.1	22.8
	IK02119	hydrozincite	−4.9	21.9
	IK02136	dolomite	2.1	21.1
	IK02150	dolomite	3.5	20.1
	IK02134	dolomite	1.6	22.4
Chah-Talkh, Iran [16]	CT-2221	hydrozincite	−7.03	9.65
	CT-2261	hydrozincite	−8.57	14.99
	CT-2211	hydrozincite	−4.91	15.15
	CT-2232	hydrozincite	−7.95	10.66
	CT-2262	hydrozincite	−8.68	7.57
	CT-2233	hydrozincite	−7.79	14.60
	CT-2212	hydrozincite	−4.88	7.80
	CT-2222	hydrozincite	−6.84	11.65
	CT-2231	hydrozincite	−9.32	14.27
	CT-2213	hydrozincite	−5.25	14.19
Kuhbanan-Bahabad, Iran [22]				
Tajkouh		smithsonite	−6.69	23.21
Tapa Sorkh		smithsonite	−1.45	21.82
Gavar		smithsonite	−7.248	23.81
Gojer		smithsonite	−4.47 to −5.43	25.65 to 26.44

Table 1. *Cont.*

Locality	Sample n.	Sample Description	$\delta^{13}C$ (‰ VPDB)	$\delta^{18}O$ (‰ VSMOW)
Angouran, Iran [4] Stage I	B15A-B	smithsonite	4.95	18.33
	B15A-R	smithsonite	5.09	21.44
	B15B-G	smithsonite	5.51	23.58
	B15B1-A	smithsonite	4.19	20.76
	B15B1-B	smithsonite	4.89	21.89
	B15B1-C	smithsonite	5.70	20.41
	B15B1-D	smithsonite	5.43	22.26
	B15-1	smithsonite	5.91	21.00
	B15-3	smithsonite	5.86	20.65
	B15A-M	smithsonite	4.74	20.29
	B3-1	smithsonite	4.33	18.87
	B3-2	smithsonite	4.60	21.02
	B13R	smithsonite	4.25	20.45
	B13A	smithsonite	4.74	21.73
	B14-1	smithsonite	6.00	20.59
	B14-2	smithsonite	5.84	21.26
	AA0	smithsonite	4.32	20.99
	AA37B	smithsonite	4.24	19.42
	AA37A	smithsonite	3.21	22.71
	AT-1A	smithsonite	5.83	22.16
	AT-7A	smithsonite	3.96	20.51
Stage II	B15B-B	smithsonite	4.62	24.92
	AT-3A	smithsonite	3.08	24.33
	AT-4A	smithsonite	−0.78	24.93
Jabali, Yemen [10]	125-32-3b	smithsonite	−4.92	21.08
	125-32-3c	smithsonite	−5.71	20.78
	125-30-1b	smithsonite	−5.48	20.70
	125-30-1c	smithsonite	−4.85	20.56
	J125-32-3c	smithsonite	−4.69	20.71
	J125-30-1c-A	smithsonite	−5.22	20.69
	J125-32-2c	smithsonite	−4.83	21.38
	J125-30-1c-B	smithsonite	−5.47	20.62
	125-10-2a	smithsonite	−4.16	20.03
	J125-15-1d	smithsonite	−4.68	19.09
	J125-9-7e	smithsonite	−3.75	19.33
	J125-10-1a	smithsonite	−3.40	19.70
	J125-14-5c	smithsonite	−2.88	19.10

Note: significant figures are reported in this table as in the original papers.

4.1. Turkey

The $\delta^{13}C$ values of Hakkari smithsonite 1 range between −3.4 and −5.8‰ V-PDB, whereas their $\delta^{18}O$ values are less variable, ranging between 24.2 and 24.6‰ V-SMOW. The unique sample of smithsonite 2 has a more negative $\delta^{13}C$ (−6.0‰ V-PDB) and a more positive $\delta^{18}O$ (25.4‰ V-SMOW) than smithsonite 2 [8]. The $\delta^{18}O$ compositions of the host rock limestone are around 24.9‰ V-SMOW, whereas their $\delta^{13}C$ values range from −0.7‰ to −2.5‰. Sparry calcite from veins cutting the host rock shows a limited range in $\delta^{18}O$ and $\delta^{13}C$, with values between 21.4 and 21.6‰ V-SMOW, and −1.8 and −2.0‰ V-PDB, respectively. Sparry calcite cogenetic with smithsonite shows similar $\delta^{18}O$ values as the calcite from the veins (21.5 and 22.6‰ V-SMOW), but substantially lower $\delta^{13}C$ ratios (−5.9 and −7.4‰ V-SMOW) [8].

The $\delta^{13}C$ values of the Hakkari host rock limestone are in a range typical for Late Jurassic carbonates [28], whereas the $\delta^{18}O$ values are significantly lower, pointing to diagenetic modifications. Calcite precipitated together with supergene smithsonite shows compositions typical of terrestrial carbonates [29]. The $\delta^{13}C$ values of smithsonite are interpreted as a result of mixing between carbonate carbon from the host rock and soil/atmospheric CO_2. The $\delta^{18}O$ values of smithsonite are in the characteristic range of supergene smithsonite encountered in other ore districts of the world [15]. As outlined by Gilg et al. [15], the $\delta^{18}O$ of smithsonite is dependent on temperature during Zn carbonate formation and on $\delta^{18}O$ of ambient waters, with the $\delta^{18}O$ of the host limestone not influencing the

oxygen isotope composition of the newly formed Zn carbonate. If the $\delta^{18}O$ of the solution from which smithsonite was formed can be approximated, the precipitation temperature can be calculated using the equation [15]

$$1000 \ln \alpha_{\text{smithsonite-water}} = 3.10 \cdot (10^6/T^2) - 3.50$$

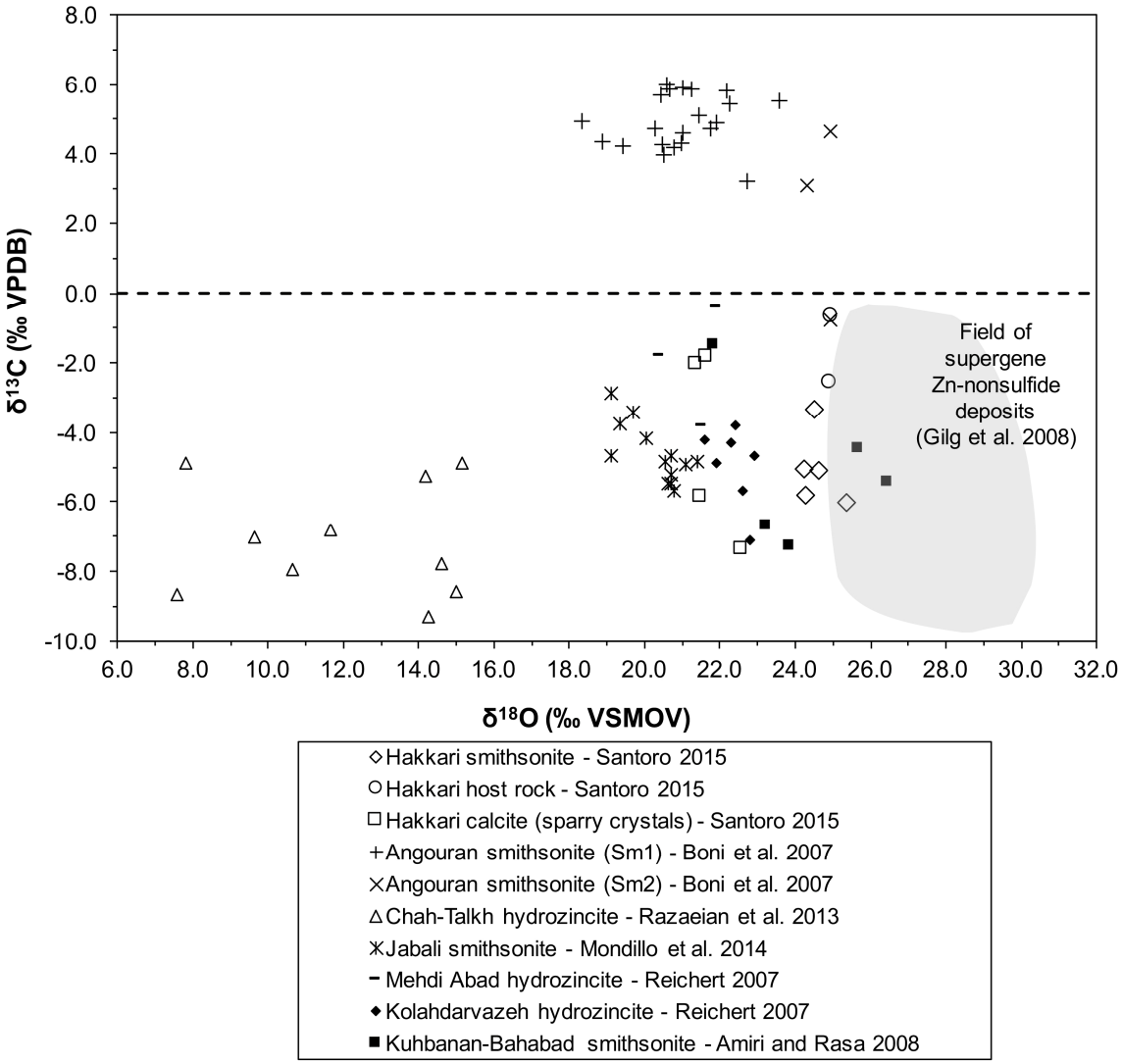

Figure 2. Carbon and oxygen isotope values of smithsonite, hydrozincite, and calcite from several occurrences in the Middle East.

Modern spring waters collected in two different areas around Hakkari have an oxygen isotope composition between −9.8‰ and −10.0‰ V-SMOW [30]. The $\delta^{18}O$ values, measured in the fluid inclusions of Pleistocene to Holocene speleothems from karstic caves of eastern central Turkey, point to an oxygen isotope composition of drip waters that range between −14.5 and −11‰ V-SMOW [30]. If the Hakkari smithsonite was formed from a fluid with a $\delta^{18}O$ value comparable to modern groundwater, the precipitation temperature would have been between ~10 and ~18 °C. If smithsonite was instead precipitated from a fluid with a $\delta^{18}O$ value comparable to Pleistocene to Holocene cave water, the precipitation temperature would have been below 10 °C. Even if the latter temperatures seem to be too low for the current climate in southeastern Turkey, they are in agreement with the data published by Rowe et al. [31], who calculated a Holocene and Late Glacial Maximum temperature

from ~4 to ~13 °C, using the equation of McDermott et al. [32]. The above temperatures correspond thus to a normal weathering environment in that time at this latitude.

4.2. Iran

Carbon and oxygen isotope measurements were applied to hydrozincite, dolomite, and limestone host rock samples of the Mehdi Abad mine [5]. However, the hydrozincite samples were said not to have a monomineralic composition, being a mixture of hydrozincite and smithsonite. The same limitation is also valid for the hydrozincite samples from the Kolahdarvazeh mine (Irankuh) [5]. The limestone samples show a restricted range of both $\delta^{13}C$ (between 2.2 and 2.9‰) and $\delta^{18}O$ values (between 22.4 and 25‰), which correspond to the typical interval of Cretaceous marine limestone [33]. The hydrozincite samples are in an interval of $\delta^{18}O$ values, between 20.4 and 21.9‰. The $\delta^{13}C$ values are more variable and range between −3.8 and −0.4‰. The latter signature is similar to that of supergene smithsonites, published by Gilg et al. [15]. It indicates that at least two isotopically different sources of carbon contributed to the formation of zinc carbonates in this part of Iran. The variably low-to-medium-depleted $\delta^{13}C$ values reflect the influence of meteoric water associated with subaerial exposure, and point to the precipitation of the zinc carbonates within the vadose and/or phreatic zone [3,5]. The isotopically light component of the carbon is the result of dissolved CO_2 derived from the decay of organic matter [5,34]. The $\delta^{18}O$ values of hydrozincites, however, are lower than the common supergene values of the smithsonites comprised in the field of Gilg et al. [15].

The hydrozincite samples measured at Kolahdarvazeh show a range of $\delta^{18}O$ V-SMOW values between 21.9 and 22.9‰ that are very similar to those measured in Mehdi Abad. The $\delta^{13}C$ values range between −7.1 and −3.8‰, which are up to 3.3‰ lower than those from hydrozincite of Mehdi Abad [5]. The formation of hydrozincite should be potentially influenced by an isotopically light component of carbon, as a result of dissolved CO_2 derived from the decay of organic matter. Since hydrozincite of the Kolahdarvazeh mine shows lower $\delta^{13}C$ values than its pendant from Mehdi Abad, a more important role of organic and meteoric CO_2 is suggested for Kolahdarvazeh in respect to Mehdi Abad.

In the Chah-Talkh deposit, the measured oxygen and carbon isotope composition of hydrozincite resulted in $\delta^{13}C$ and $\delta^{18}O$ values ranging from −9.3 to −4.9‰ V-PDB and from 7.6 to 15.2‰ V-SMOW, respectively [16]. Comparing the oxygen and carbon isotope data with published parameters of rocks and waters from different geological environments, Rezaeian et al. [16] observed that the $\delta^{18}O$ values of the Chah-Talkh hydrozincite have the same $\delta^{18}O$ composition of metamorphic host rocks, and suggested an influence of metamorphic waters during nonsulfide mineralization. The authors also considered the low oxygen isotope values as related to high temperature fluids, and calculated a formation temperature of ~80 to 100 °C for hydrozincite [16]. Carbon and oxygen isotopes of smithsonite in the deposits of the Kuhbanan–Bahabad area range from −7.25 to −1.45‰ V-PDB and from 21.82 to 26.44‰ V-SMOW, respectively [22]. From this district, only the smithsonite sample from Tapa Sorkh has an anomalous composition ($\delta^{13}C$ = −1.45‰ V-PDB and $\delta^{18}O$ = 21.82‰ V-SMOW). Smithsonites from other deposits in the area (Tajkouh, Gavar, Goier) have compositions similar to smithsonites occurring in other supergene deposits. Following Amiri and Rasa [22], these data apparently show that the fluids responsible for the formation of smithsonite were "a combination of basinal (connate) fluids, ground waters and meteoric waters".

Stable isotope measurements of the carbonates were quite revealing for the genesis of Angouran nonsulfide ores [4]. Smithsonite from stage I displays variable $\delta^{18}O$ values ranging from 18.3 to 23.6‰ V-SMOW, while its carbon isotope composition is fairly constant and unusually high (3.2 to 6.0‰ V-PDB), with an average value of ~4.9‰ V-PDB [4]. In contrast, smithsonite from stage II ores shows a much smaller range of $\delta^{18}O$ values (from 24.3 to 24.9‰ V-SMOW), but lower $\delta^{13}C$ values over a considerable spread (−0.8 to 4.6‰ V-PDB). Assuming an oxygen isotope composition of waters identical to that of the present-day hot springs in the Takab area ($\delta^{18}O_{water}$ = −10‰ V-SMOW), a formation temperature between 15 and 40 °C was calculated by Boni et al. [4] for stage I smithsonite. Consequently, it was suggested that these kinds of Zn-carbonates were formed in a low-temperature

hydrothermal system, most probably related to several stages of Tertiary–Quaternary volcanic activity. The co-precipitation of smithsonite with galena, pyrite, and arsenopyrite [4,6], as well as the absence of Fe- and Mn-oxides/hydroxides and of any discernible oxidation or dissolution of the primary sulfide ore, shows that the fluids responsible for the stage I carbonate ores were relatively reduced, and close to neutral to slightly basic pH with high fCO_2. The carbon did not originate locally from the Angouran marble wall-rock bearing $\delta^{13}C$ values of +2‰, but from a deeper, hotter source [4,15]. The similarity between the heavy carbon isotope compositions of stage I smithsonite and those of some of the hot-spring travertines in the Takab region, suggested that the positive $\delta^{13}C$ was a "product of very high temperature decarbonatization (which might be related to contact metamorphism) and low-temperature deposition (<100 °C)" [4]. The carbon and oxygen isotope signatures (constant oxygen and variable and light carbon isotope values) of stage II smithsonite are compatible with a supergene origin of this carbonate mineral: in fact, the ample spread of $\delta^{13}C$ indicates the presence of organic soil CO_2 as second C source, whereas the high $\delta^{18}O$ value suggests a decrease of smithsonite precipitation temperature [4,15].

4.3. Yemen

Smithsonite in the nonsulfide section of the Jabali deposit has a $\delta^{18}O$ composition that varies between 19.1 and 21.4‰ V-SMOW. The $\delta^{13}C$ values are always negative, in a range between −5.7 and −2.9‰ V-PDB [10]. The $\delta^{18}O$ spread of the smithsonite values was interpreted as due to: (i) precipitation from a low-temperature hydrothermal system; or (ii) precipitation from supergene waters with a variable $\delta^{18}O$ ratio. The associated negative $\delta^{13}C$ composition was considered to be related to a mixing of carbon from host rock carbonates and soil/atmospheric CO_2 into meteoric-surficial waters, involved in a deep thermal circulation [10].

5. Discussion and Conclusions

Carbon and oxygen stable isotopes analyses of smithsonite have shown that the Hakkari (Turkey) nonsulfide ore deposit was formed through the precipitation of Zn-carbonates from low-temperature fluids, after supergene weathering and oxidation of a primary sulfide mineralization [8]. The same genesis has been suggested for the Mehdi Abad and Irankuh nonsulfides (Iran) [5,22], even though the oxygen isotopic ratios of hydrozincite from these deposits are outside the compositional range of the typical supergene smithsonites elsewhere. A comparable isotopic behavior has been observed in the hydrozincites of the Mina Grande nonsulfide deposit in Peru [35], which have on average $\delta^{18}O$ values 2 to 3 points‰ lower than the corresponding smithsonites. However, since no smithsonite has been measured at Mehdi Abad and Irankuh, the considered hydrozincite samples in both deposits were not pure [5], and the mineral-water oxygen fractionation factor of hydrozincite has not yet been determined, it would not be correct to directly compare the hydrozincite values with the isotopic data of smithsonite from the other deposits considered. In the Chah-Talkh deposit, hydrozincite $\delta^{18}O$ compositions, exceptionally lower than compositions measured in any other nonsulfide deposit of the world [15,16], were interpreted suggesting mineral precipitation from metamorphic waters at a temperature of ~80 to 100 °C [16]. However, the texture of hydrozincite described in [16] ("the smithsonite mineral is in the form of microcrystalline and in most parts has transformed to hydrozincite, which forms cryptocrystalline mass"), which is typical of hydrozincite formed from very surficial waters [14,15], makes difficult to believe to a genesis related to metamorphic fluids. In our opinion the Chah-Talkh hydrozincite more likely formed from mixtures of strongly ^{16}O-enriched meteoric waters, characterized by very negative $\delta^{18}O$ compositions. The Tajkouh, Gavar, and Goier deposits, located in the Kuhbanan–Bahabad area present smithsonites characterized by compositions indicating a supergene origin. Only the smithsonite sample from Tapa Sorkh has a high $\delta^{18}O$ composition (21.82‰ V-SMOW), which could be produced either by "a combination of basinal (connate) fluids, ground waters and meteoric waters" [22], or by ^{18}O-depleted meteoric waters. The $\delta^{18}O$ composition of smithsonite in the Jabali deposit (Yemen) is

much lower than in other smithsonites in known supergene deposits [10,11], whereas its carbon isotope composition is in the same range of the negative $\delta^{13}C$ values recorded in most supergene nonsulfide ores [15]. It was therefore assumed that the Jabali smithsonite precipitated through different stages from a combination of fluids consisting of local groundwaters variably mixed with low-temperature hydrothermal waters [10].

In conclusion, if we compare the C–O isotopic signatures of Zn-carbonates of nonsulfide Zn deposits in the Middle East, it becomes obvious that only few of them can be considered beyond doubt as genetically associated with supergene weathering fluids. This means that, even though all these mineralizations are uniformly classified as "Nonsulfide Zn deposits", they cannot be grouped into a single genetic model. For example, most Zn-carbonates at Angouran (Iran) were deposited from hydrothermal fluids associated with late magmatism, as the travertine deposits in the same area, and the Jabali (Yemen) secondary ores were again deposited from a low-temperature hydrothermal system. Consequently, when looking for nonsulfide Zn deposits in the Middle East, it is necessary to consider that, in addition to simple weathering, other mechanisms may have been responsible for the genesis of this type of ores and, therefore, the exploration philosophy might be correspondingly adapted. As shown in the paper, C–O stable isotopes geochemistry is useful to discriminate among different genetic mechanisms involved in the formation of Zn nonsulfide deposits, and if routinely adopted when studying smithsonite-bearing mineralization, it could be a powerful tool to better focus the exploration strategies also at a regional scale.

Acknowledgments: The authors are indebted to the Assistant Editor for handling the paper, and to the anonymous reviewers for discussion and suggestions. This research was carried out with Departmental funds (University of Napoli Federico II) to M. Boni and N. Mondillo.

Author Contributions: Nicola Mondillo and Maria Boni wrote the manuscript. Michael Joachimski analyzed the C-O stable isotopes of the carbonates. Licia Santoro supported N. Mondillo and M. Boni for data compilation and discussion.

Conflicts of Interest: The authors declare no conflict of interest.

References

1. Reynolds, N.; Large, D. Tethyan zinc-lead metallogeny in Europe, North Africa, and Asia. *Econ. Geol. Spec. Publ.* **2010**, *15*, 339–365.
2. Yigit, O. Mineral deposits of Turkey in relation to Tethyan metallogeny: Implications for future mineral exploration. *Econ. Geol.* **2009**, *104*, 19–51. [CrossRef]
3. Borg, G. Geological and economical significance of supergene nonsulphide zinc deposits in Iran and their exploration potential. In Proceedings of the 20th World Mining Congress Geological Survey of Iran (ed) Mining and Sustainable Development, Tehran, Iran, 7–11 November 2005; pp. 385–390.
4. Boni, M.; Gilg, H.A.; Balassone, G.; Schneider, J.; Allen, C.R.; Moore, F. Hypogene Zn carbonate ores in the Angouran deposit, NW Iran. *Miner. Depos.* **2007**, *42*, 799–820. [CrossRef]
5. Reichert, J. A Metallogenetic Model for Carbonate-Hosted Non-Sulphide Zinc Deposits Based on Observations of Mehdi Abad and Irankuh, Central and Southwestern Iran. Ph.D. Thesis, Martin-Luther-Universität Halle-Wittenberg, Halle, Germany, 2007; p. 152.
6. Daliran, F.; Pride, K.; Walther, J.; Berner, Z.A.; Bakker, R.J. The Angouran Zn(Pb) deposit, NW Iran: Evidence for a two stage, hypogene zinc sulfide zinc carbonate mineralization. *Ore Geol. Rev.* **2013**, *53*, 373–402. [CrossRef]
7. Santoro, L.; Boni, M.; Herrington, R.; Clegg, A. The Hakkari nonsulfide Zn-Pb deposit in the context of other nonsulfide Zn–Pb deposits in the Tethyan Metallogenic Belt of Turkey. *Ore Geol. Rev.* **2013**, *53*, 244–260. [CrossRef]
8. Santoro, L. The Jabali, Hakkari and Reef Ridge nonsulfide Zn(Pb) Deposits: An Evaluation by QEMSCAN®Technology, and Comparison to Other Analytical Methods. Ph.D. Thesis, Università degli Studi di Napoli "Federico II", Napoli, Italy, 2015; p. 276.

9. Santoro, L.; Rollinson, G.K.; Boni, M.; Mondillo, N. Automated Scanning Electron Microscopy (QEMSCAN®) based mineral identification and quantification of the Jabali Zn-Pb-Ag nonsulfide deposit (Yemen). *Econ. Geol.* **2015**, *110*, 1083–1099. [CrossRef]
10. Mondillo, N.; Boni, M.; Balassone, G.; Joachimski, M.; Mormone, A. The Jabali Nonsulfide Zn-Pb-Ag Deposit, Western Yemen. *Ore Geol. Rev.* **2014**, *61*, 248–267. [CrossRef]
11. Boni, M.; Mondillo, N. The "Calamines" and the "Others": The great family of supergene nonsulfide zinc ores. *Ore Geol. Rev.* **2015**, *67*, 208–233. [CrossRef]
12. Movahednia, M.; Rastad, E.; Rajabi, A.; Choulet, F. Mineralogy, geochemistry and genetic processes of supergene non-sulphide ore of the Ab-Bagh Sedimentary-Exhalative (SEDEX-type) Zn-Pb deposit, Sanandaj-Sirjan zone. *Geosciences* **2017**, *26*, 249–264.
13. Large, D. The geology of nonsulfide zinc deposits—An overview. *Erzmetall* **2001**, *54*, 264–274.
14. Hitzman, M.W.; Reynolds, N.A.; Sangster, D.F.; Allen, C.R.; Carman, C. Classification, genesis, and exploration guides for nonsulfide zinc deposits. *Econ. Geol.* **2003**, *98*, 685–714. [CrossRef]
15. Gilg, H.A.; Boni, M.; Hochleitner, R.; Struck, U. Stable isotope geochemistry of carbonate minerals in supergene oxidation zones of Pb-Zn deposits. *Ore Geol. Rev.* **2008**, *33*, 117–133. [CrossRef]
16. Rezaeian, A.; Rasa, I.; Amiri, A.; Jafari, M.R. Stable isotope (O and C) geochemistry of nonsulfide Zn–Pb deposits; case study: Chah-Talkh nonsulfide Zn–Pb deposit (Sirjan, south of Iran). *Arab. J. Geosci.* **2014**, *7*, 2329–2338. [CrossRef]
17. Ceyhan, N. Lead Isotope Geochemistry of Pb-Zn Deposits from Eastern Taurides, Turkey. Master's Thesis, Graduate School of Natural and Applied Sciences of the Middle East Technical University, Ankara, Turkey, 2003; p. 105.
18. Yilmaz, A.; Ünlü, T.; Sayili, I.S. An approach to the origin of Keban Lead-Zinc Mineralizations, Elaziğ, Turkey: A preliminary study. *Miner. Res. Expl. Bull.* **1992**, *114*, 27–50.
19. Venter, M.; Robertson, M. *Desktop, Remote Sensing and Field Validation*; Internal Report; Red Crescent Resources A.Ş.: Ankara, Turkey, 2009.
20. Maghfouri, S.; Hosseinzadeh, M.R.; Rajabi, A.; Choulet, F. A review of major non-sulfide zinc deposits in Iran. *Geosci. Front.* **2017**, 1–25, in press.
21. Maghfouri, S.; Hosseinzadeh, M.R.; Rajabi, A.; Azimzadeh, A.M.; Choulet, F. Geology and origin of mineralization in the Mehdiabad Zn-Pb-Ba (Cu) deposit, Yazd Block, Central Iran. In Proceedings of the 13th SGA Biennial Meeting, Nancy, France, 24–27 August 2015.
22. Amiri, A.; Rasa, I. The non-sulfide ore formation conditions of Ravar-Bafgh area, findings of carbon and oxygen stable isotopes. *Quart. Appl. Geol.* **2008**, *3*, 95–103. (In Farsi)
23. Gilg, H.A.; Boni, M.; Balassone, G.; Allen, C.R.; Banks, D.; Moore, F. Marble-hosted sulfide ores in the Angouran Zn-(Pb-Ag) deposit, NW Iran: Interaction of sedimentary brines with a metamorphic core complex. *Miner. Depos.* **2006**, *31*, 1–16. [CrossRef]
24. Al Ganad, I.; Lagny, P.; Lescuyer, J.L.; Rambo, C.; Touray, J.C. Jabali, a Zn-Pb-(Ag) carbonate-hosted deposit associated with Late Jurassic rifting in Yemen. *Miner. Depos.* **1994**, *29*, 44–56. [CrossRef]
25. Boni, M.; Mondillo, N.; Balassone, G. Zincian dolomite: A peculiar de-dolomitization case? *Geology* **2011**, *39*, 183–186. [CrossRef]
26. Rosenbaum, J.; Sheppard, S.M. An isotopic study of siderites, dolomites and ankerites at high temperatures. *Geochim. Cosmochim. Acta* **1986**, *50*, 1147–1150. [CrossRef]
27. Kim, S.T.; Mucci, A.; Taylor, B.E. Phosphoric acid fractionation factors for calcite and aragonite between 25 °C and 75 °C: Revisited. *Chem. Geol.* **2007**, *246*, 135–146. [CrossRef]
28. Jenkyns, H.C.; Jones, C.E.; Gröcke, D.R.; Hesselbo, S.P.; Parkinson, D.N. Chemostratigraphy of the Jurassic System: Application, limitations and implications for palaeoceanography. *J. Geol. Soc. Lond.* **2003**, *159*, 351–378. [CrossRef]
29. Boni, M.; Gilg, H.A.; Aversa, G.; Balassone, G. The "Calamine" of SW Sardinia (Italy): Geology, mineralogy and stable isotope geochemistry of a supergene Zn-mineralization. *Econ. Geol.* **2003**, *98*, 731–748. [CrossRef]
30. Mutlu, H.; Güleç, N.; Hilton, D.R.; Aydin, H.; Halldórsson, S.A. Spatial variation in gas and stable isotope compositions of thermal fluids around Lake Van: Implications for crust-mantle dynamics Turkey. *Chem. Geol.* **2012**, *300*, 165–176. [CrossRef]

31. Rowe, P.J.; Mason, J.E.; Andrews, J.E.; Marca, A.D.; Thomas, L.; Van Calsteren, P.; Jex, C.N.; Vonhof, H.B.; Al-Omari, S. Speleothem isotopic evidence of winter rainfall variability in northeast Turkey between 77 and 6 ka. *Quat. Sci. Rev.* **2012**, *45*, 60–72. [CrossRef]
32. McDermott, F. Palaeo-climate reconstruction from stable isotope variations in speleothems: A review. *Quat. Sci. Rev.* **2006**, *23*, 901–918. [CrossRef]
33. Veizer, J.; Hoefs, J. Nature of O^{18}/O^{16} and C^{13}/C^{12} secular trends in sedimentary carbonate rocks. *Geoch. Cosm. Acta* **1976**, *40*, 387–395. [CrossRef]
34. Cerling, T.E. The stable isotopic composition of modern soil carbonate and its relationship to climate. *Earth Planet. Sci. Lett.* **1984**, *71*, 229–240. [CrossRef]
35. Arfè, G.; Mondillo, N.; Boni, M.; Balassone, G.; Joachimski, M.; Mormone, A.; Di Palma, T. The karst hosted Mina Grande nonsulfide zinc deposit, Bongará district (Amazonas region, Peru). *Econ. Geol.* **2017**, *112*, 1089–1110. [CrossRef]